Characterisation of renal cell carcinoma-associated constitutional chromosome abnormalities by genome sequencing

Philip S Smith (1), James Whitworth (1), Hannah West (1), Jacqueline Cook (2), Carol Gardiner (3), Derek Lim (4), Patrick J Morrison (5), R. Gordon Hislop (6), Emily Murray (6), NIHR Rare Disease BioResource (7), Marc Tischkowitz (1), Anne Y Warren (8), Emma R Woodward (9), Eamonn R Maher (1)

1) Department of Medical Genetics, University of Cambridge and NIHR Cambridge Biomedical Research Centre, and Cancer Research UK Cambridge Centre, Cambridge Biomedical Campus, Cambridge CB2 0QQ, UK

2) Department of Clinical Genetics, Sheffield Children's Hospital, Sheffield, UK

3) West of Scotland Genetics Services, Queen Elizabeth University Hospital, Glasgow, UK

4) West Midlands Regional Genetics Service, Birmingham Women's and Children's National Health Service (NHS) Foundation Trust, Birmingham, UK

5) Northern Ireland Regional Genetics Service, Belfast City Hospital, Belfast Health & Social Care Trust, Belfast, UK

6) Ninewells Hospital, University of Dundee, Dundee, UK

7) NIHR BioResource, Cambridge University Hospitals, Cambridge Biomedical Campus, Cambridge CB2 0QQ, UK

8) Department of Histopathology, Cambridge University NHS Foundation Trust and Cancer Research UK Cambridge Centre, Cambridge CB2 OQQ, United Kingdom

9) Manchester Centre for Genomic Medicine and NW Laboratory Genetics Hub, Manchester University Hospitals NHS Foundation Trust, and Division of Evolution and Genomic Sciences, School of Biological Sciences, Faculty of Biology, Medicine and Health, University of Manchester, Health Innovation Manchester, Manchester, UK.

Correspondence to:

Professor Eamonn Maher, Department of Medical Genetics, University of Cambridge, Box 238, Cambridge Biomedical Campus, Cambridge, CB2 0QQ, United Kingdom

E-mail: erm1000@medschl.cam.ac.uk

Telephone: 01223 746714

Fax: 01223 746777

Abstract

Constitutional translocations, typically involving chromosome 3, have been recognised as a rare cause of inherited predisposition to renal cell carcinoma (RCC) for four decades. However, knowledge of the molecular basis of this association is limited. We have characterised the breakpoints by genome sequencing (GS) of constitutional chromosome abnormalities in five individuals who presented with RCC. In one individual with constitutional t(10;17)(q11.21;p11.2) the translocation breakpoint disrupted two genes: the known renal tumour suppressor gene (TSG) *FLCN* (and clinical features of Birt-Hogg-Dubé syndrome were detected) and *RASGEF1A*. In four cases the rearrangement breakpoints did not disrupt known inherited RCC genes. In the second case without chromosome 3 involvement the translocation breakpoint in an individual with a constitutional t(2;17)(q21.1;q11.2) mapped 12 Kb upstream of *NLK*. Interestingly NLK has been reported to interact indirectly with FBXW7 and a previously reported RCC-associated translocation breakpoint disrupted *FBXW7*. In two cases of constitutional chromosome 3 translocations, no candidate TSGs were identified in the vicinity of the breakpoints. However in an individual with a constitutional chromosome 3 inversion the 3p breakpoint disrupted the *FHIT* TSG (which has been reported previously to be disrupted in two apparently unrelated families with a RCC-associated t(3;8)(p14.2;q24.1). These findings a) expand the range of constitutional chromosome rearrangements that may be associated with predisposition to RCC, b) confirm that chromosome rearrangements not involving chromosome 3 can predispose to RCC, c) suggest that a variety of molecular mechanisms are involved the pathogenesis of translocation associated RCC and d) demonstrate the utility of genome sequencing for investigating such cases.

Introduction

Kidney cancer accounts for almost 2% of new cancer diagnoses globally and the incidence increased by 36% between 1990 and 2013 [1]. The most common form of kidney cancer in adults is renal cell carcinoma (RCC) which is histologically and genetically heterogeneous. Approximately 3% of cases of RCC are recognised as having a genetic basis and a variety of syndromic and non-syndromic forms of RCC have been delineated [2]. Although familial forms of RCC are infrequent, the identification of the molecular basis of inherited RCC, as exemplified by von Hippel-Lindau (VHL; MIM 193300) disease, has been crucial to understanding the molecular mechanisms of sporadic cases of RCC [3]. In addition to *VHL*, germline mutations in multiple other genes have been reported to predispose to RCC including *BAP1, FH, FLCN, MET, PTEN, SDHB, SDHD, SDHA, SDHC* [2,4]. Furthermore constitutional translocations, particularly those involving chromosome 3, have been associated with inherited RCC in multiple reports.

Four decades ago, Cohen *et al.* (1979) described a large kindred in which clear cell RCC segregated with a constitutional translocation between the short arm of chromosome 3 and the long arm of chromosome 8, t(3;8)(p14.2;q24.1), such that the risk of RCC in translocation carriers was estimated to be 80% at age 60 years [5]. Subsequently somatic deletions of the short arm of chromosome 3 (3p) were found to be the most common cytogenetic abnormality in sporadic clear cell RCC suggesting the presence of critical renal tumour suppressor genes on 3p [6]. These developments led to the suggestion that identification of individuals with suspected inherited forms of RCC should be screened for constitutional translocations involving 3p and that the characterisation of RCC-associated translocation breakpoints might lead to the identification of novel inherited RCC genes [7]. Subsequent research studies have confirmed that the short arm of chromosome 3 does indeed harbour several tumour suppressor genes (TSGs) that are frequently inactivated in sporadic RCC (e.g. *VHL, PBRM1, BAP1, RASSF1A*) [8–15].

In a review of previously published reports, we identified 17 RCC-associated constitutional translocations (15 of which involved a chromosome 3 breakpoint) of constitutional chromosome abnormalities associated with RCC (Table 1) [7,16–29]. Molecular characterisation of the translocation breakpoints in individual cases have identified a series of candidate TSGs disrupted (or nearby) the translocation breakpoints (Table 4 & 5) but none of the 15 cases with chromosome 3 breakpoints were found to disrupt either 3p genes that are frequently mutated in sporadic RCC or known familial RCC genes that map outside of 3p (e.g. *FLCN, FH, SDHB*). The observation that the chromosome 3 breakpoints in RCC-associated translocations were heterogeneous led to the suggestion that RCC predisposition in such cases might not necessarily involve disruption of a TSG but might confer susceptibility because of instability of the derivative chromosome 3 leading to loss at an early stage of tumourigenesis [30].

Assessment and characterisation of further families and individuals carrying translocations associated with predisposition to RCC may help elucidate the genetic features and mechanisms that lead to disease onset in these patients. Here, we report the results of performing genome sequencing (GS) to characterise five constitutional rearrangements detected in individuals with RCC and interpret the results in the context of previous reports of RCC-associated constitutional translocations.

Materials and Methods

Literature review

Reports of cases of RCC with a constitutional chromosome rearrangement were identified through a search of PubMed using the search terms "renal cell carcinoma" or "renal cancer" or "kidney cancer/tumour" and "rearrangement/inversion/translocation or chromosome" and by searching of previously published reports (performed January 2019). When previous reports had suggested candidate genes that were either close to or disrupted by the relevant chromosomal breakpoints, evidence to suggest that the genes were implicated in human cancer was sought by reviewing curated data from the Network of Cancer Genes data portal (NCG; http://ncg.kcl.ac.uk/ version 6) [31] (performed January 2019) where genes were classified as either 'known cancer genes', 'candidate cancer genes', or 'non-cancer genes'. Genes flagged as 'false positive cancer genes' were designated as 'non-cancer genes'.

Clinical studies

Individuals presenting with RCC and with constitutional rearrangements were ascertained through Regional Clinical Genetics Units in the United Kingdom. DNA was extracted from whole blood according to standard protocol in the referring genetics service and, when available, paraffin embedded tumour material was obtained from the relevant hospital histopathology department. All patients gave written informed consent and the study was approved by the South Birmingham Ethics Committee.

Sequence alignment and variant calling

DNA from four probands was sequenced at Novogene. A total of >1µg gDNA (1.2 – 1.7µg) at approximately 100ng/µl was used for genome sequencing (30X coverage). Generated FASTQ files were aligned to GRCh38 using BWA mem (version 0.7.15-r1140) [32]. BAM files were sorted, PCR duplicates removed, and indexed, after which Indel realignment and base score recalibration was performed using GATK IndelRealigner and BaseRecalibrator (version 3.7-0-gcfedb67)[33], respectively. Genome-wide variant calling was jointly performed on all samples using GATK unified genotyper (version 3.7-0-gcfedb67) (33). DNA from one proband underwent GS as part of the NIHR BioResource Rare Diseases study with sequencing and primary bioinformatics performed as previously described[34]. Data were aligned to genome build GRCh37 and all analyses were performed identically with appropriate adjustments for differences in genome build. All genomic coordinates are reported in GRCh38 and GRCh37 coordinates were remapped using the NCBI remap tool (https://www.ncbi.nlm.nih.gov/genome/tools/remap). Called SNVs were processed and filtered for various quality control metrics and allelic frequency (supplemental table 1).

Genome sequencing analysis: Candidate gene analysis and Breakpoint identification

The GS results were analysed for evidence for rare, potentially pathogenic, SNVs and copy number abnormalities in previously reported inherited RCC genes (*VHL, MET, FH, SDHB, SDHD, SDHC, BAP1, CDKN2B*) [2,4]. Copy number detection was performed using Canvas Copy Number Variant Caller (version 1.39.0.1598)[35], copy number variants were filtered to include calls only marked as "PASS". Structural rearrangements and breakpoints were identified using Manta Structural Variant Caller (version 1.3.1)[36]. Manta structural variants were filtered to include only calls marked as "PASS", number of supporting spanning/split reads > 5, QUAL > 100, and call frequency (Supplemental table S3). Full details of bioinformatic processes are described in the supplemental material. Breakpoints called on chromosomes matching cytogenetic reports were visually inspected using Integrative Genomics Viewer (IGV – version 2.3.93) to confirm the presence of split and spanning reads (Supplemental figures S1-5). The data that support the findings of this study are available from the corresponding author upon reasonable request.

Topologically-associated domain analysis

TADs reported by Dixon *et al.* derived from human embryonic stem cells (GRCh38) were used as the reference TAD set [37] at 40 kb resolution. Structural variation coordinates were intersected with TAD coordinates using bedtools (version 2.25.0) [38]. The corresponding TADs were then intersected with the genomic positions of all known gene loci [39](Supplemental information) to find genes contained within a given TAD and only protein-coding genes were included. Protein-coding genes identified within a TAD were assessed for potential function in cancer using the Network of Cancer Genes data portal (NCG; http://ncg.kcl.ac.uk/ version 6) [31], as previously described. TAD regions were visualised using the Hi-C data browser (http://promoter.bx.psu.edu/hi-c/index.html) [40].

Sanger sequencing

Direct sequencing of breakpoints was performed by Sanger sequencing using breakpoint spanning primer pairs (Supplemental table S2). PCR products were generated using Amplitaq Gold polymerase (Applied Biosystems – CA, USA) following the manufacturer's protocol. PCR products were sequenced using the BigDye™ Terminator v3.1 Cycle Sequencing Kit (Applied Biosystems – CA, USA) following the manufacturer's protocol. Termination sequencing products were purified by isopropanol precipitation, re-suspended in Hi-Di Formamide (Applied Biosystems – CA, USA), and sequenced on the ABI 3730 sequencing platform (Applied Biosystems – CA, USA). Sequences were aligned and analysed using Sequencher DNA analysis software (version 5.3.4; Gene Codes – MI, USA).

Statistical tests

All statistical tests were performed using R project for statistical computing (version 3.5.1). Welch's t-test was performed using the package BSDA (version 1.2.0) with the function tsum.test. Kruskal–Wallis rank sum test was performed using the base R function kruskal.test. Fisher's exact test was performed using the base R function fisher.test. Statistical testing was undertaken on data from confirmed translocation carriers only.

Results

Literature Review of Previously Reported Cases

A total of 17 previously published distinct constitutional chromosome rearrangements were identified from searches of the biomedical literature (Table 1). In 15 cases (88%) chromosome 3 was involved (all of which were reciprocal translocations) and there were a variety of partner chromosomes in the 15 translocation cases (e.g. three with chromosome 6, three with chromosome 8 – Table 1 and Figure 1). For the RCC-associated chromosome 3 translocation cases, the breakpoints were almost evenly distributed between the long arm (3q, n=8) and short arm (3p; n=7) and were heterogeneous (Figure 2).

Review of the clinical and pathological data in the previously reported cases demonstrated 9 kindreds with at least 2 related individuals with RCC. In the 4 cases without a family history and available clinical information, multiple RCCs were described in 2 individuals. The mean age at diagnosis of a renal tumour in those cases known to carry a constitutional chromosomal rearrangement was 50 years (range 25-82 years). Histopathological details were available for 43 cases and clear cell RCC was reported in 42 (98%) cases.

Previous studies have demonstrated that cases of sporadic and familial RCC differ by mean age of diagnosis, with RCC presenting earlier in familial cases [41,42]. Comparison of the mean age of diagnosis of RCC in translocation cases to familial and sporadic RCC cases (as reported previously by Maher *et al.*[41] & Woodward *et al*[42]) were 50.2 (SD=12.7), 48.2 (SD=12.3), and 61.8 (SD=10.8) years of age, respectively. Translocation cases have a statistically lower age of diagnosis than those with sporadic disease (Welch's t-test, $p=9.84 \times 10^{-7}$) but no significant difference between translocation and familial cases was observed (Welch's t-test, p=0.522). Though age of diagnosis across all affected translocation carriers is variable there was no significant difference in age between familial (with 2 or more related individuals) translocation cases (Kruskal–Wallis test, p=0.174).

The chromosomal rearrangement breakpoints had been mapped in 15 of 17 previously reported cases and a total of 10 candidate genes had been reported to be disrupted by the relevant rearrangement breakpoints (Table 4). Additionally, 21 genes found to be in the vicinity of translocation breakpoints and cited as relevant genes by the authors of the original report were also assessed (Table 5).The evidence for implicating the various genes in RCC predisposition was assessed using NCG data portal (Table 4 & 5). Of the 10 genes directly disrupted by translocation breakpoints, two are classified as known cancer genes, with all remaining genes having no evidence supporting their role in cancer. In regards to 21 genes stated to be in the vicinity of a translocation breakpoint, 2 were designated as known cancer genes and 4 were classified as candidate cancer genes.

Clinical Features of Previously Unreported Cases

Five previously unreported constitutional chromosomal rearrangements ascertained through a patient presenting with RCC were identified through UK genetics services. The cytogenetic, clinical features and pathological features of the five probands and (where relevant) their affected relatives are described in Table 2. There were 4 translocations (involving chromosome 3 in two cases) and a pericentric inversion of chromosome 3 (Table 2 and Figure 1). Two or more individuals developed RCC in three kindreds.

In the kindred with the t(3;14)(q13.3;q22) 6 individuals developed RCC (three of whom were confirmed or obligate translocation carriers). The proband presented with bilateral clear cell RCC at age 75 years, his daughter died from RCC at age 36 years, his mother and two of his brothers were reported to have developed RCC at ages 51, 41 and 79 years respectively. The proband's brother was an obligate t(3;14)(q13.3;q22) carrier and his son developed RCC at age 67 years and was confirmed to be a translocation carrier.

In the kindred with the t(3;6)(p14.2;p12) rearrangement, the proband presented with RCC at age 72 years and four relatives were demonstrated to also harbour the translocation. Three had not developed RCC (age at last follow up 47-52 years) but one (the proband's brother) had developed bilateral clear cell RCC at age 55 years with unilateral recurrent disease and an adrenal metastasis at age 74 years and his son died from RCC at age 40 years without any record of his status for the t(3;6)(p14.2;p12) translocation.

The index case in whom the inv(3)(p21.1q12) was identified was unaffected but was ascertained following a report that her cousin had developed clear cell RCC at age 39 and harboured the chromosome 3 inversion. Other unaffected carriers of the inversion in the family included her paternal aunt and father, whilst her grandfather was also to be a carrier and died of carcinomatosis around age 80 years. The proband's brother was diagnosed with RCC at age 48 but was not tested for the inversion.

The t(2;17)(q21;q11.2) was identified in a 37 year old man with a poorly differentiated in part clear cell RCC who died from metastatic disease shortly thereafter. The translocation was maternally inherited and was detected in three unaffected family members (mother and two siblings) aged between 30 and 58 years of age.

In the kindred with the t(10;17)(q11.22;p12) the proband, with his sister, were found to have features of suggestive Birt-Hogg-Dubé syndrome (BHD; MIM 135150) (pneumothoraces, and fibrofolliculomas in the proband and multiple pulmonary cysts and fibrofolliculomas in the sister) after the diagnosis of RCC in the proband and the detection of the translocation.

Molecular Characterisation of Constitutional Rearrangements in Previously Unreported Cases

Genome sequencing did not identify any plausible likely pathogenic or pathogenic SNVs or CNVs in previously reported inherited RCC genes (V*HL, SDHB, SDHC, SDHD, MET, FLCN, TSC1, TSC2, FH, PTEN, PBRM1, BAP1* and *CDKN2B*) in the four probands who were affected by RCC (the index case with the inv(3)(p21.1q12) had a family history of RCC but had not developed RCC). A novel missense

variant of uncertain significance by ACMG criteria [43] was identified in *PBRM1* (NM_018313.4:c.2446A>T p.Asn816Tyr) in the t(3;6)(p14.2;p12) case. DNA from an affected individual was not available for sequencing in the family carrying the inv(3)(p21.1q12), as such sequencing was performed solely to identify candidate breakpoints. Candidate rearrangement breakpoints were identified from the GS data by the Manta structural variation detection algorithm in all five cases.

Breakpoints for translocation t(3;14)(q13.3;q22) were resolved to be present at the loci chr3:125771297 and chr14:59009871-59009875. The candidate breakpoints were supported by 7 and 9 spanning and split reads, respectively (Supplemental table 2). The candidate breakpoint locations identified by GS differed from those suggested previously by cytogenetic studies. The 3q breakpoint at chr3:125771297 is within cytoband 3q21 and the GS-identified 14q breakpoint at chr14:59009871 maps to 14q23 with respective genomic distances of 7.3 Mb and 4.7 Mb from the reported cytogenetic bands seen by karyotyping. Sanger sequencing confirmed the presence of the translocation breakpoints. Sanger sequencing in a DNA sample from his affected nephew confirmed identical breakpoints to the proband. The 3q breakpoint intersects with *LOC105374312*, an uncharacterised non-coding RNA gene and the 14q breakpoint disrupts the last intron of *LINC01500*, a long intergenic non-coding RNA gene, and is predicted to result in a truncated transcript lacking the final exon.

GS in the second chromosome 3 associated translocation case t(3;6)(p14.2;p12) revealed candidate breakpoints at chr3:66680663 and chr6:54817716 within an AT-rich repetitive region. Breakpoint calls were supported by 4 and 7 spanning and split read calls, respectively (Supplemental table 2). Discordance between karyotyping and GS-derived cytoband positions was limited to adjacent bands with 3p14.2 being mapped to 3p14.1 (5.5 Mb centromeric) and 6p12 being defined at a greater resolution at 6p12.1. Sanger sequencing confirmed the presence of the translocation breakpoints. The 3p chromosomal breakpoint identified by GS mapped within 3p14.1 and disrupted LOC105377142, an uncharacterised non-coding RNA. The 6p breakpoint did not disrupt a predicted gene but was 29 kb upstream of *FAM83B* in 6p12.1.

The candidate breakpoints in the inv(3)(p21.1q12) were identified by Manta with 11 spanning and 11 split reads supporting the presence of this inversion, though the number of reference spanning reads was only 2 (Supplemental table 2). The two candidate breakpoints mapped to chr3:59964935 at 3p14.2 (interrupting intron 7 of *FHIT*) and chr3:98667603 at 3q12 (47 kb upstream of *ST3GAL6-AS1*, a non-coding RNA gene). The discrepancy between the cytogenetic position and GS-derived positions did not greatly deviate from other differences seen in other cases with the 3p breakpoint at 3p21 detected 6.6 Mb closer to the centromere at 3p14.2. Though cytogenetics and Manta calls support the presence of the inv(3)(p14.2q12), Sanger sequencing under multiple experimental conditions failed to generate any PCR products and the candidate breakpoints could not be independently confirmed.

Assessment of the DNA at the described breakpoints for the inv(3)p14.2q12) rearrangement was performed to determine if local DNA features and nucleotide composition may explain the failure to confirm the inversion by Sanger sequencing. Analysis of each breakpoint within a $\pm$1 Kb window demonstrated a lower than average GC-content percentage at both sites (chr3:59963935-59965935 = 32.3% and chr3:98666603-98668603 = 36.6%) compared to genome-wide GC content. Furthermore, the 3p14.2 breakpoint occurred within proximity of two repeat elements (chr3:59965304-59965360-(AT)n and chr3:59965818-59965936-L3) and the 3q12 breakpoint overlapped with a repetitive region (chr3:98667322-98667927-L1M2), as well as in proximity of five further repetitive DNA elements, as defined by RepeatMasker. Taken together, particularly when considering the calling of multiple breakpoints by Manta, low complexity and additional undetermined structural variation at either one or both breakpoints may explain the failure to confirm the breakpoints by Sanger sequencing.

GS in the first of the two non-chromosome 3 translocations t(2;17)(q21;q11.2) localised the breakpoints to chr2:130693728 (2q21.1) and chr17:28030855 (17q11.2). The translocation breakpoint was supported by 9 spanning and 10 split reads as called by Manta (Supplemental table 2). Sanger sequencing confirmed the genomic coordinates and breakpoint as a single base translocation without local rearrangement, insertions, or deletions. Cytogenetic positions were inconsistent for chromosome 2 (q21) with the NGS breakpoint occurring in the adjacent band q21.1, proximately 5.3 Mb closer to q telomere. The breakpoint present on chromosome 2 disrupted the coding region of two overlapping pseudogenes *KLF2P3* and *FAR2P3*, as well as interrupting a CpG island spanning chr2:130693485-130693839. The nearest coding genes were *POTEJ*, *AMER3*, and *GPR148* which were 35 kb upstream, 34 kb downstream and 62 kb downstream, respectively. The junction on chromosome 17 did not disrupt any known coding region but was 1.7 kb upstream of a reported H3K27Ac element spanning chr17:28,033,593-28,035,092, and 9.9 kb upstream of the *NLK* gene.

The second non-chromosome 3 translocation t(10;17)(q11.22;p12) underwent sequencing as part of the NIHR BioResource Rare Diseases BRIDGE project (see methods) and was analysed previously as part of a multiple primary tumour cohort [34] with a history of facial fibrofolliculomas, recurrent pneumothoraces and renal cell carcinoma. At that time no abnormality was detected but subsequently reanalysis identified candidate translocation breakpoints that were supported by two overlapping Manta calls for the chromosome 10 and chromosome 17 breakpoints at chr17:17218211-17218214 (17p11.2) and chr10:43236047-43236050 (10q11.21) that were supported by 22 spanning and 10 split reads and a secondary call at chr17:17218216-17218217 and chr10:43236058-43236059 by 15 spanning and 18 split reads (Supplemental table S2). As with other cases, differences between breakpoints on chromosome 10 and 17 from both karyotyping and GS were found with 10q11.22 mapping to 10q11.21 (3.3 Mb centromeric) and 17p12 mapping to 17p11.2 (3.7 Mb centromeric). Given the proximity of the assigned breakpoint regions, a single translocation was presumed with an additional nested structural variation resulting in divided calling. Sanger sequencing confirmed the presence of the translocation breakpoint in the proband. The chromosome 17 breakpoint prediction disrupted the coding region of *FLCN*, falling within intron 9 (ENST00000285071). The chromosome 10 breakpoint disrupted the first intron of *RASGEF1A* (the first exon encodes the 5' untranslated region proximal to the translation initiation site (ENST00000395810). The proband's sibling, who was known to carry the t(10;17)(q11.22;p12), was also found to have evidence of BHD syndrome (multiple lung and renal cysts and facial fibrofolliculomas).

While RNA was not available for the t(10;17)(q11.21;p11.2) proband to assess fusion gene formation, both genes are on the negative strand and do not appear to interrupt splice site consensus sequences, suggesting fusion gene products could be transcribed consisting of exon 1 of *RASGEF1A* with exons 10-14 of *FLCN* and exons 1-9 of *FLCN* with exons 2-13 of *RASGEF1A*, from each derivative chromosome respectively.

Translocations as determined by karyotyping, next generation sequencing cytobands (NGS), standardised nomenclature, and cytoband discrepancies are noted in Table 3. Translocations will be referred to by the shortened nomenclature system as described by Ordulu *et al.* [44] in both the text and tables hereafter.

Computational evaluation of breakpoint-related genes

The five constitutional rearrangements were confirmed or postulated to disrupt three protein coding genes (*FHIT, FLCN* and *RASGEF1A*). Two of these genes, *FHIT* and *FLCN,* have been previously implicated as renal tumour suppressor genes [45,46] and the NCG data portal classified both *FHIT* and *FLCN* as "known cancer genes", *RASGEF1A* as a "candidate cancer gene".

Assessment of the effect of a translocation on the surround genomic architecture and consequently the impact on gene regulation is more challenging. Within the nucleus, DNA is rearranged into complex two dimensional and three dimensional structures, and this spatial organisation directly impacts biological

function. Higher order chromatin structures such as topologically associated domains (TADs) have been identified as pervasive and highly conserved features of genome organisation [47] and that disruption of these TADs and their associated genomic boundaries can lead to gene dysfunction, ectopic genomic interactions, and disease phenotypes [48,49]. We sort to assess if any breakpoints occurred within topologically associated domains and to what extent, if any, these disruptions could dysregulate long range gene regulatory structures.

A total of 8/10 rearrangement breakpoints occurred within a TAD (or a TAD boundary region), with the chromosome 3 breakpoint in t(3;14)(q21;q23) and chromosome 2 breakpoint in t(2;17)(q21.1;q11.2) occurring within "unorganized chromatin" regions (Table 6 and supplemental figures S7-S16). TADs which harboured a breakpoint were assessed for encapsulated genes and the subsequently identified genes assessed for relevance to cancer via the NCG (Table 6). Analysis demonstrated two known cancer genes (*NCOA4* and *RET*) and a further five candidate cancer genes (*LLGL1*, *LRIG1*, *LYRM9*, *ST3GAL6*, and *TMEM199*) were within breakpoint-containing TADs.

Tumour Analysis

Tumour material was available for an affected individual with the familial t(3;14)(q21;q23), and expert histopathological review classified the two separate tumours (A=3 cm and B=3.8 cm) for which material was received as clear cell RCC. Tumour A was classed as WHO/ISUP Grade 2 B (as focal grade but predominantly grade 2). No necrosis was seen. Immunohistochemistry on sections from Tumour B demonstrated staining of moderate intensity with CA-IX and AE1/3 and weak focal staining with vimentin. Only rare cells were CK7 positive and the tumour was negative for CD117, HMB45 and Mel-A, an immunoprofile consistent with the diagnosis.

Using a NGS sequencing panel of 68 cancer-related genes, as described previously [50], tumour sequencing was performed on the two renal tumours to assess *VHL* mutation state. The larger tumour harboured a frameshift deletion in *VHL* (NM_000551: c.408delT: p.Phe136Leufs*23: rs397516442) in 49% of reads but no somatic mutations in *VHL* were detected in the smaller tumour. Analysis of the other genes on the sequencing panel did not demonstrate any protein-affecting somatic alteration either tumour at a variant allele fraction greater than 10%.

Sufficient DNA was available for one of the t(3;14)(q21;q23) tumours (tumour B, 38 mm diameter) to perform genome-wide copy number assessment using the Applied Biosystems OncoScan CBV FFPE assay kit as described previously.[68] The OncoScan assay identified chromosomal alterations consistent with the loss of the der(3), including 3p, and retention of the wild type chromosomes (3 and 14) and der(14) (arr[GRCh37] 3p26.3q21.2(63410-125495356)x1,(5)x3,14q23.1q32.33(59491095-107282024)x1,(X)x1). Additionally, the tumour also harboured trisomy 5 and loss of chromosome Y (Supplemental information and supplemental figures 17 & 18).

Discussion

We describe five previously unreported RCC-associated constitutional chromosomal rearrangements that increase the total number of rearrangements reported to 22 and the number of cases in which the breakpoints have been characterised to 20. We found that GS enabled both the identification of candidate translocation breakpoints and simultaneously excluded coincidental pathogenic SNVs and CNVs in known hereditary cancer genes. With the increasing availability and decreasing cost of GS it will become increasingly feasible to characterise the molecular pathology of RCC-associated constitutional chromosomal rearrangements. This will improve our understanding of the relevance to individual RCC-associated constitutional chromosomal rearrangements to the RCC tumourigenesis and we found that the breakpoint location reported on routine cytogenetic analysis often did not correspond to the breakpoint locations identified by GS. The majority (21/22, 95.5%) of RCC-associated constitutional chromosomal rearrangements reported to date have been associated with the clear cell variant of RCC. This is the most common histological subtype of sporadic RCC (75-80%) and is characterised by somatic inactivation of *VHL* and deletions of the short arm of chromosome 3 [8,9,15,51]. The mean age at diagnosis of RCC in the cases reported to date (51 years, range 25-82, n=57, SD=13.25) is younger than the average age for sporadic RCC (e.g. 61.8 years) [41]. Whilst this is a feature of other forms of hereditary RCC (and many other inherited cancer types) there may also be an element of ascertainment bias with early onset cases more likely to be investigated for a genetic cause. In the largest family we identified, t(3;14)(q21;q23), the mean age at diagnosis of RCC in the 6 affected cases was 58 years and 3 individuals were either known or obligate translocation carriers. While the breakpoints characterised by this translocation do not disrupt any known cancer gene, given the loss of the derivative chromosomes is reported as the potential initiator of tumourigenesis in chromosome 3 translocations, the loss of der(3) would also result in the loss of 14q that would include the *HIF1A* coding region, which is a candidate 14q TSG [52].

In both our own and the previously published literature series, most RCC-associated constitutional chromosome rearrangements involved chromosome 3. Whilst this is consistent with the high frequency of 3p allele loss in sporadic clear cell RCC, the fundamental role of somatic inactivation of the *VHL* TSG in clear cell RCC and the incidence of somatic mutations of *PBRM1*, *BAP1* and *SETD2* in RCC, to date most RCC-associated constitutional chromosome 3 rearrangements do not appear to disrupt known RCC TSGs mapping to 3p. A potential explanation for this is the observation that RCC from individuals with a constitutional chromosome 3 translocation can show a somatic *VHL* mutation on the wild-type chromosome 3 and loss of the derivative chromosome containing 3p (resulting in biallelic inactivation of the *VHL* TSG). This mechanism of tumourigenesis would imply that the susceptibility to RCC might result from instability of the translocated chromosome rather than disruption of a specific RCC TSG at the translocation breakpoint on chromosome 3 [30] and would be consistent with the variability of the RCC-associated chromosome 3 rearrangement breakpoints described to date (Table 1). Indeed, analysis of the larger of the larger of the two t(3;14)(q21;q23)-associated RCC revealed a somatic truncating *VHL* mutation and copy number alterations consistent with loss the of der(3) translocated chromosome that included 3p as described previously [30]. Nevertheless, it is interesting that the chromosome 3 inversion we described was associated with a breakpoint within *FHIT*. Previously it was demonstrated in two apparently unrelated families with an RCC-associated t(3;8)(p14.2;q24.1) were reported to have harboured breakpoints that disrupted *FHIT* and *RNF139* (*TRC8)* on 3p and 8q respectively [16,27]. *FHIT* is listed as a Tier 1 known cancer gene in the Cancer Gene Census (https://cancer.sanger.ac.uk/cosmic/census); however, the presence of a somatic VHL mutation and loss of the translocated chromosome 3 in a previous t(3;8)(p14.2;q24.1)-associated RCC was unexpected [5,27].

It is possible that the recurrent involvement of *FHIT* in RCC-associated chromosome 3 rearrangements reflects the presence of palindromic AT-rich repeats at the t(3;8)(p14.2;q24.1) breakpoint and causes a propensity to recurrent rearrangements at this locus [53], although we note that only a fraction of chromosome 3 translocations are associated with predisposition to RCC [54]. It is therefore conceivable that both instability of the translocated chromosome and monoallelic inactivation of *FHIT* contribute to RCC susceptibility. Analysis previously reported genes associated with translocations, as described by previous authors, and examination of TAD structures in current series identified several genes that have been previously reported to be located at or close to the breakpoints of RCC-associated chromosome 3 rearrangements (Table 4-6). These genes were reviewed to determine which were included in recently compiled lists of known cancer genes which are based on the results of recent large scale cancer genomics projects; 8 genes (*FHIT, LRIG1, FBXW7, CCNE1, STAG1, SEMA5B, PDZRN3, and HSPB8*) were identified as known or candidate cancer genes from previous publications. In addition, genes that were disrupted (*FHIT*, *FLCN, and RASGEF1A*) or occurred within a relevant TAD structure coinciding with the breakpoints of the novel RCC-associated rearrangements reported here were also assessed. A total of ten genes that were disrupted or within breakpoint associated TAD structures were classified as known (*FHIT, FLCN, NCOA4,* and *RET)* or candidate cancer genes (*LLGL1*, *LRIG1*, *LYRM9*, *RASGEF1A, ST3GAL6*, and *TMEM199*) (Table 6). The independent occurrence of *LRIG1* in two separate cases (t(3;6)(p14.1;p12.1) in this series and in Meléndez *et al.*[27]) is notable. Neither translocation directly disrupted the coding region of *LRIG1* but have occurred within the TAD (or in close proximity in the case of the latter) of the gene. *LRIG1* is known to encode a cell surface protein (Leucine-rich repeats and immunoglobulin-like domains 1; LRIG1) which is known to negatively regulate epidermal growth factor receptor (EGFR) [55] and ERBB-family receptor degradation including RET and MET [56,57], and deletions of *LRIG1* occur somatically in RCC cases at a rate of 2.3% within the TCGA dataset [15], of which 94% were clear cell RCC.

Relatively few RCC-associated constitutional translocations not involving chromosome 3 have been reported. In addition to the two novel cases reported here, there are two previously reported cases [20,21] and the translocation breakpoints were characterised in only one of these cases. It is entirely possible that non-chromosome 3 constitutional translocations and RCC might occur coincidentally and we note that, though there was an early age at onset (37 years) in the proband with t(2;17)(q21.1;q11.2) and an unconfirmed family history of RCC in his paternal grandfather, the translocation was also found in his mother and two siblings who were unaffected at ages 58, 40 and 31 years. However, identification of a translocation breakpoint that disrupted the *FLCN* gene in a patient with a t(10;17)(q11.21;p11.2) illustrated the value of characterising all RCC-associated constitutional rearrangements. Inactivating mutations in *FLCN* cause BHD syndrome which is characterised by facial fibrofolliculomas, pulmonary cysts and pneumothorax and RCC [45,58]. The occurrence of fibrofolliculomas is age-dependent and pneumothorax occurs in a minority of cases and so BHD may present with non-syndromic RCC [59]. However in the family reported herein the t(10;17)(q11.21;p11.2) was associated with other evidence of BHD syndrome. To our knowledge this is the first description of a constitutional translocation causing BHD syndrome.

The other novel translocation case did not disrupt a known cancer gene but occurred close to *NLK* (Nemo-Like Kinase) a serine/threonine-protein kinase, which has been associated with the non-canonical Wnt and MAPK signalling pathways. Whilst *NLK* is currently not designated as a known cancer gene, evidence of tumour suppressor activity has been reported [60–62] and a role for NLK in the stabilisation of p53 has been suggested [63]. Interestingly, NLK appears to collaborate with FBXW7 in the ubiquitination of c-Myb by enhancing ligation of additional ubiquitin molecules via NLK phosphorylation, leading to downregulation of cellular proliferation [64] and, previously, an RCC-associated constitutional translocation, t(3;4)(q21;q31), was demonstrated to interrupt *FBXW7* [18]. Furthermore, *FBXW7* is a designated tumour suppressor gene that is mutated in multiple types of primary cancers and encodes an F-box protein that is part of a SCF complex thought to target cyclin E and mTOR for ubiquitin-mediated degradation [65,66]. Very recently *FBXW7* has been identified as a novel cancer predisposition gene following an analysis of individuals with Wilms tumour [67]. Additionally, it was demonstrated that FBXW7 interacts with Ubiquitin-conjugating enzyme E2Q-like protein 1 (UBE2QL1), the gene is known to be disrupted in a previously reported RCC translocation case [21], suggesting an interesting connection between multiple interacting gene products in translocation-related RCC.

In conclusion, we report five new cases of RCC-associated constitutional chromosome rearrangements characterised by GS. These include the first example of a chromosome 3 inversion associated with RCC, the first case of a major inherited RCC gene disrupted by a translocation and a third example of a RCC constitutional chromosome rearrangement that disrupts *FHIT*. Review of the five novel cases reported here and previously reported cases demonstrates that RCC-associated constitutional chromosome rearrangements 1) mostly involve chromosome 3 but rearrangements that solely involve other chromosomes may also be causally linked to RCC, 2) may predispose to RCC by a variety of mechanisms including disruption of a tumour suppressor gene (e.g. *FLCN*) and/or chromosomal instability (as with chromosome 3 translocations), 3) can be efficiently characterised by GS and 4) can identify candidate pathways for RCC tumourigenesis. For chromosome 3 translocations it is unclear why most cases that are not ascertained because of a personal or family history of RCC appear to be associated with a very low risk of RCC [54]. In those translocations that do predispose to RCC there may be a combination of factors involved including instability of the translocated chromosome during cell division together with disruption of a TSG (e.g. *FHIT*) and/or polygenic effects that increase RCC susceptibility.

Acknowledgements

Conflict of Interest Statement

The authors do not have any conflicts of interest to declare.

References

1. Fitzmaurice C, Dicker D, Pain A, et al. The Global Burden of Cancer 2013. *JAMA Oncol*. 2015;1(4):505. doi:10.1001/jamaoncol.2015.0735
2. Maher ER. Genomics and epigenomics of renal cell carcinoma. *Semin Cancer Biol*. 2013;23(1):10-17. doi:10.1016/j.semcancer.2012.06.003
3. Gossage L, Eisen T, Maher ER. VHL, the story of a tumour suppressor gene. *Nat Rev Cancer*. 2015;15(1):55-64. doi:10.1038/nrc3844
4. Shuch B, Zhang J. Genetic Predisposition to Renal Cell Carcinoma: Implications for Counseling, Testing, Screening, and Management. *J Clin Oncol*. 2018;36(36):3560-3566. doi:10.1200/JCO.2018.79.2523
5. Cohen AJ, Li FP, Berg S, et al. Hereditary renal-cell carcinoma associated with a chromosomal translocation. *N Engl J Med*. 1979;301(11):592-595. doi:10.1056/NEJM197909133011107
6. Zbar B, Brauch H, Talmadge C, Linehan M. Loss of alleles of loci on the short arm of chromosome 3 in renal cell carcinoma. *Nature*. 1987;327(6124):721-724. doi:10.1038/327721a0
7. Boldog FL, Gemmillt RM, Wilkes CM, et al. Positional cloning of the hereditary renal carcinoma 3;8 chromosome translocation breakpoint (suppresor gene/fagile site/polycystic kidney diease/lung cancer/thyroid cancer). *Genetics*. 1993;90:8509-8513.
8. Foster K, Prowse A, van den Berg A, et al. Somatic mutations of the von Hippel-Lindau disease tumour suppressor gene in non-familial clear cell renal carcinoma. *Hum Mol Genet*. 1994;3(12):2169-2173.
9. Gnarra JR, Tory K, Weng Y, et al. Mutations of the VHL tumour suppressor gene in renal carcinoma. *Nat Genet*. 1994;7(1):85-90. doi:10.1038/ng0594-85
10. Young AC, Craven RA, Cohen D, et al. Analysis of VHL Gene Alterations and their Relationship to Clinical Parameters in Sporadic Conventional Renal Cell Carcinoma. *Clin Cancer Res*. 2009;15(24):7582-7592. doi:10.1158/1078-0432.CCR-09-2131
11. Varela I, Tarpey P, Raine K, et al. Exome sequencing identifies frequent mutation of the SWI/SNF complex gene PBRM1 in renal carcinoma. *Nature*. 2011;469(7331):539-542. doi:10.1038/nature09639
12. Peña-Llopis S, Vega-Rubín-de-Celis S, Liao A, et al. BAP1 loss defines a new class of renal cell carcinoma. *Nat Genet*. 2012;44(7):751-759. doi:10.1038/ng.2323
13. Dreijerink K, Braga E, Kuzmin I, et al. The candidate tumor suppressor gene, RASSF1A, from human chromosome 3p21.3 is involved in kidney tumorigenesis. *Proc Natl Acad Sci U S A*. 2001;98(13):7504-7509. doi:10.1073/pnas.131216298
14. Morrissey C, Martinez A, Zatyka M, et al. Epigenetic inactivation of the RASSF1A 3p21.3 tumor suppressor gene in both clear cell and papillary renal cell carcinoma. *Cancer Res*. 2001;61(19):7277-7281.
15. Network CGAR, N. J, Weinstein JN, et al. The Cancer Genome Atlas Pan-Cancer analysis project. *Nat Genet*. 2013;45(10):1113-1120. doi:10.1038/ng.2764
16. Gemmill RM, West JD, Boldog F, et al. The hereditary renal cell carcinoma 3;8 translocation fuses FHIT to a patched-related gene, TRC8. *Proc Natl Acad Sci U S A*. 1998;95(16):9572-9577.
17. Bonne A, Vreede L, Kuiper RP, et al. Mapping of constitutional translocation breakpoints in renal cell cancer patients: identification of KCNIP4 as a candidate gene. *Cancer Genet Cytogenet*. 2007;179(1):11-18. doi:10.1016/j.cancergencyto.2007.07.005
18. Kuiper RP, Vreede L, Venkatachalam R, et al. The tumor suppressor gene FBXW7 is disrupted by a constitutional t(3;4)(q21;q31) in a patient with renal cell cancer. *Cancer Genet Cytogenet*. 2009;195(2):105-111. doi:10.1016/j.cancergencyto.2009.07.001
19. McKay L, Frydenberg M, Lipton L, Norris F, Winship I. Case report: renal cell carcinoma segregating with a t(2;3)(q37.3;q13.2) chromosomal translocation in an Ashkenazi Jewish family. *Fam Cancer*. 2011;10(2):349-353. doi:10.1007/s10689-010-9413-y
20. Doyen J, Carpentier X, Haudebourg J, et al. Renal cell carcinoma and a constitutional t(11;22)(q23;q11.2): case report and review of the potential link between the constitutional t(11;22) and cancer. *Cancer Genet*. 2012;205(11):603-607. doi:10.1016/j.cancergen.2012.09.006
21. Wake NC, Ricketts CJ, Morris MR, et al. UBE2QL1 is disrupted by a constitutional translocation associated with renal tumor predisposition and is a novel candidate renal tumor suppressor gene. *Hum Mutat*. 2013;34(12):1650-1661. doi:10.1002/humu.22433
22. Yusenko M V., Nagy A, Kovacs G. Molecular analysis of germline t(3;6) and t(3;12) associated with conventional renal cell carcinomas indicates their rate-limiting role and supports the three-hit model of carcinogenesis. *Cancer Genet Cytogenet*. 2010;201(1):15-23.
23. Chen J, Lui W-O, Vos MD, et al. The t(1;3) breakpoint-spanning genes LSAMP and NORE1 are involved in clear cell renal cell carcinomas. *Cancer Cell*. 2003;4(5):405-413. doi:10.1016/S1535-6108(03)00269-1
24. Eleveld MJ, Bodmer D, Merkx G, et al. Molecular analysis of a familial case of renal cell cancer and a t(3;6)(q12;q15). *Genes, Chromosom Cancer*. 2001;31(1):23-32. doi:10.1002/gcc.1114
25. Druck T, Podolski J, Byrski T, et al. The DIRC1 gene at chromosome 2q33 spans a familial RCC-associated t(2;3)(q33;q21) chromosome translocation. 2001;46(10):583-589. doi:10.1007/s100380170025
26. Bodmer D, Eleveld M, Kater-Baats E, et al. Disruption of a novel MFS transporter gene, DIRC2, by a familial

renal cell carcinoma-associated t(2;3)(q35;q21). *Hum Mol Genet*. 2002;11(6):641-649.

27. Meléndez B, Rodríguez-Perales S, Martínez-Delgado B, et al. Molecular study of a new family with hereditary renal cell carcinoma and a translocation t(3;8)(p13;q24.1). *Hum Genet*. 2003;112(2):178-185. doi:10.1007/s00439-002-0848-6

28. Poland KS, Azim M, Folsom M, et al. A constitutional balanced t(3;8)(p14;q24.1) translocation results in disruption of theTRC8 gene and predisposition to clear cell renal cell carcinoma. *Genes, Chromosom Cancer*. 2007;46(9):805-812. doi:10.1002/gcc.20466

29. Foster RE, Abdulrahman M, Morris MR, et al. Characterization of a 3;6 translocation associated with renal cell carcinoma. *Genes Chromosomes Cancer*. 2007;46(4):311-317. doi:10.1002/gcc.20403

30. Bodmer D, Eleveld MJ, Ligtenberg MJL, et al. An Alternative Route for Multistep Tumorigenesis in a Novel Case of Hereditary Renal Cell Cancer and a t(2;3)(q35;q21) Chromosome Translocation. *Am J Hum Genet*. 1998;62:1475-1483.

31. Repana D, Nulsen J, Dressler L, et al. The Network of Cancer Genes (NCG): a comprehensive catalogue of known and candidate cancer genes from cancer sequencing screens. *Genome Biol*. 2019;20(1):1. doi:10.1186/s13059-018-1612-0

32. Li H, Durbin R. Fast and accurate short read alignment with Burrows-Wheeler transform. *Bioinformatics*. 2009;25(14):1754-1760. doi:10.1093/bioinformatics/btp324

33. McKenna A, Hanna M, Banks E, et al. The Genome Analysis Toolkit: a MapReduce framework for analyzing next-generation DNA sequencing data. *Genome Res*. 2010;20(9):1297-1303. doi:10.1101/gr.107524.110

34. Whitworth J, Smith PS, Martin J-E, et al. Comprehensive Cancer-Predisposition Gene Testing in an Adult Multiple Primary Tumor Series Shows a Broad Range of Deleterious Variants and Atypical Tumor Phenotypes. *Am J Hum Genet*. 2018;103(1):3-18. doi:10.1016/j.ajhg.2018.04.013

35. Roller E, Ivakhno S, Lee S, Royce T, Tanner S. Canvas: versatile and scalable detection of copy number variants. *Bioinformatics*. 2016;32(15):2375-2377. doi:10.1093/bioinformatics/btw163

36. Chen X, Schulz-Trieglaff O, Shaw R, et al. Manta: rapid detection of structural variants and indels for germline and cancer sequencing applications. *Bioinformatics*. 2016;32(8):1220-1222. doi:10.1093/bioinformatics/btv710

37. Dixon JR, Jung I, Selvaraj S, et al. Chromatin architecture reorganization during stem cell differentiation. *Nature*. 2015;518(7539):331-336. doi:10.1038/nature14222

38. Quinlan AR, Hall IM. BEDTools: A flexible suite of utilities for comparing genomic features. *Bioinformatics*. 2010;26(6):841-842. doi:10.1093/bioinformatics/btq033

39. Smedley D, Haider S, Durinck S, et al. The BioMart community portal: an innovative alternative to large, centralized data repositories. *Nucleic Acids Res*. 2015;43(W1):W589-W598. doi:10.1093/nar/gkv350

40. Wang Y, Song F, Zhang B, et al. The 3D Genome Browser: A web-based browser for visualizing 3D genome organization and long-range chromatin interactions. *Genome Biol*. 2018;19(1). doi:10.1186/s13059-018-1519-9

41. Maher ER, Yates JR, Ferguson-Smith M a. Statistical analysis of the two stage mutation model in von Hippel-Lindau disease, and in sporadic cerebellar haemangioblastoma and renal cell carcinoma. *J Med Genet*. 1990;27(5):311-314. doi:10.1136/jmg.27.5.311

42. Woodward ER, Clifford SC, Astuti D, Affara NA, Maher ER. Familial clear cell renal cell carcinoma (FCRC): clinical features and mutation analysis of the VHL, MET, and CUL2 candidate genes. *J Med Genet*. 2000;37(5):348-353. doi:10.1136/JMG.37.5.348

43. Richards S, Aziz N, Bale S, et al. Standards and guidelines for the interpretation of sequence variants: a joint consensus recommendation of the American College of Medical Genetics and Genomics and the Association for Molecular Pathology. *Genet Med*. 2015;17(5):405-423. doi:10.1038/gim.2015.30

44. Ordulu Z, Wong KE, Currall BB, et al. Describing sequencing results of structural chromosome rearrangements with a suggested next-generation cytogenetic nomenclature. *Am J Hum Genet*. 2014;94(5):695-709. doi:10.1016/j.ajhg.2014.03.020

45. Nickerson ML, Warren MB, Toro JR, et al. Mutations in a novel gene lead to kidney tumors, lung wall defects, and benign tumors of the hair follicle in patients with the Birt-Hogg-Dubé syndrome. *Cancer Cell*. 2002;2(2):157-164. doi:10.1016/S1535-6108(02)00104-6

46. Vocke CD, Yang Y, Pavlovich CP, et al. High Frequency of Somatic Frameshift BHD Gene Mutations in Birt-Hogg-Dubé-Associated Renal Tumors. *J Natl Cancer Inst*. 2005;97(12). doi:10.1093/jnci/dji154

47. Dixon JR, Selvaraj S, Yue F, et al. Topological domains in mammalian genomes identified by analysis of chromatin interactions. *Nature*. 2012;485(7398):376-380. doi:10.1038/nature11082

48. Lupiáñez DG, Spielmann M, Mundlos S. Breaking TADs: How Alterations of Chromatin Domains Result in Disease. *Trends Genet*. 2016;32(4):225-237. doi:10.1016/j.tig.2016.01.003

49. Spielmann M, Lupiáñez DG, Mundlos S. Structural variation in the 3D genome. *Nat Rev Genet*. 2018;19(7):453-467. doi:10.1038/s41576-018-0007-0

50. Casey RT, Warren AY, Rodrigues JE, et al. Clinical and Molecular Features of Renal and Phaeochromocytoma/Paraganglioma Tumour Association Syndrome (RAPTAS): Case Series and Literature Review. *J Clin Endocrinol Metab*. July 2017. doi:10.1210/jc.2017-00562

51. Banks RE, Tirukonda P, Taylor C, et al. Genetic and epigenetic analysis of von Hippel-Lindau (VHL) gene alterations and relationship with clinical variables in sporadic renal cancer. *Cancer Res*. 2006;66(4):2000-2011. doi:10.1158/0008-5472.CAN-05-3074

52. Shen C, Beroukhim R, Schumacher SE, et al. Genetic and Functional Studies Implicate HIF1 as a 14q Kidney Cancer Suppressor Gene. *Cancer Discov*. 2011;1(3):222-235. doi:10.1158/2159-8290.CD-11-0098

53. Kato T, Franconi CP, Sheridan MB, et al. Analysis of the t(3;8) of hereditary renal cell carcinoma: a palindrome-mediated translocation. *Cancer Genet*. 2014;207(4):133-140. doi:10.1016/j.cancergen.2014.03.004

54. Woodward ER, Skytte A-B, Cruger DG, Maher ER. Population-based survey of cancer risks in chromosome 3 translocation carriers. *Genes, Chromosom Cancer*. 2010;49(1):52-58. doi:10.1002/gcc.20718

55. Gur G, Rubin C, Katz M, et al. LRIG1 restricts growth factor signaling by enhancing receptor ubiquitylation and degradation. *EMBO J*. 2004;23(16):3270-3281. doi:10.1038/sj.emboj.7600342

56. Ledda F, Bieraugel O, Fard SS, Vilar M, Paratcha G. Lrig1 is an endogenous inhibitor of ret receptor tyrosine kinase activation, downstream signaling, and biological responses to GDNF. *J Neurosci*. 2008;28(1):39-49. doi:10.1523/JNEUROSCI.2196-07.2008

57. Shattuck DL, Miller JK, Laederich M, et al. LRIG1 Is a Novel Negative Regulator of the Met Receptor and Opposes Met and Her2 Synergy. *Mol Cell Biol*. 2007;27(5):1934-1946. doi:10.1128/mcb.00757-06

58. Menko FH, van Steensel MA, Giraud S, et al. Birt-Hogg-Dubé syndrome: diagnosis and management. *Lancet Oncol*. 2009;10(12):1199-1206. doi:10.1016/S1470-2045(09)70188-3

59. Woodward ER, Ricketts C, Killick P, et al. Familial Non-VHL Clear Cell (Conventional) Renal Cell Carcinoma: Clinical Features, Segregation Analysis, and Mutation Analysis of FLCN. *Clin Cancer Res*. 2008;14(18):5925-5930. doi:10.1158/1078-0432.CCR-08-0608

60. Emami KH, Brown LG, Pitts TEM, Sun X, Vessella RL, Corey E. Nemo-like kinase induces apoptosis and inhibits androgen receptor signaling in prostate cancer cells. *Prostate*. 2009;69(14):1481-1492. doi:10.1002/pros.20998

61. Yasuda J, Tsuchiya A, Yamada T, Sakamoto M, Sekiya T, Hirohashi S. Nemo-like kinase induces apoptosis in DLD-1 human colon cancer cells. *Biochem Biophys Res Commun*. 2003;308(2):227-233.

62. Han Y, Kuang Y, Xue X, et al. NLK, a novel target of miR-199a-3p, functions as a tumor suppressor in colorectal cancer. *Biomed Pharmacother*. 2014;68(5):497-505. doi:10.1016/j.biopha.2014.05.003

63. Zhang H-H, Li S-Z, Zhang Z-Y, et al. Nemo-like kinase is critical for p53 stabilization and function in response to DNA damage. *Cell Death Differ*. 2014;21(10):1656-1663. doi:10.1038/cdd.2014.78

64. Kanei-Ishii C, Nomura T, Takagi T, Watanabe N, Nakayama KI, Ishii S. Fbxw7 acts as an E3 ubiquitin ligase that targets c-Myb for nemo-like kinase (NLK)-induced degradation. *J Biol Chem*. 2008;283(45):30540-30548. doi:10.1074/jbc.M804340200

65. Koepp DM, Schaefer LK, Ye X, et al. Phosphorylation-Dependent Ubiquitination of Cyclin E by the SCFFbw7 Ubiquitin Ligase. *Science (80-)*. 2001;294(5540):173-177. doi:10.1126/science.1065203

66. Mao J-H, Kim I-J, Wu D, et al. FBXW7 targets mTOR for degradation and cooperates with PTEN in tumor suppression. *Science*. 2008;321(5895):1499-1502. doi:10.1126/science.1162981

67. Mahamdallie S, Yost S, Poyastro-Pearson E, et al. Identification of new Wilms tumour predisposition genes: an exome sequencing study. *Lancet Child Adolesc Heal*. 2019;3(5):322-331. doi:10.1016/S2352-4642(19)30018-5

68. Aird JJ, Nic An Riogh AU, Fleming S, Hislop RG, Sweeney P, Mayer N. Papillary Renal Cell Carcinoma With Osteosarcomatous Heterologous Differentiation: A Case Report With Molecular Genetic Analysis and Review of the Literature. Int J Surg Pathol. 2017;25:745-750

Table 1: Clinical features of RCC in individuals from families with a constitutional chromosome rearrangement. Individuals marked * were presumed to be carriers of the relevant rearrangement but were not tested.

Publication(s)	Cytology	Breakpoint (GRCh38)	Histology (RCC)	Type (foci = n)	Sex	Age
Cohen *et al.* [1979]	t(3;8)(pl4.2;q24.1)	N/a	Clear cell	Bilateral (n=2)	M	37
			Clear cell	Bilateral (n=3)	M	45
			Clear cell	Unilateral (n>2)	M	59
			Clear cell	Unilateral (n=3)	F	46
			Clear cell	Unilateral (n=1)	M	44
			Clear cell	Unilateral (n=1)	F	50
			Clear cell	Bilateral (n>3)	F	41
			Clear cell *	Bilateral (n>2)	M	47
			Clear cell *	Bilateral (n=9)	F	44
			Not specified	Bilateral (n=7)	F	39
Kovacs *et al.* [1988]	t(3;12)(q13.2;q24.1)	N/a	Clear cell	Unilateral (n=1)	M	50
Kovacs *et al.* [1989]	t(3;6)(p13;q25.1)	N/a	Clear cell	Bilateral (n = 5)	M	53
Koolen *et al.* [1998]	t(2;3)(q35;q21)	N/a	Clear cell	Bilateral (n=3)	M	54
			Not specified	N/a	F	53
			Clear cell	Unilateral (n=3)	F	68
			Clear cell	Unilateral (n=1)	M	40
			Clear cell	Bilateral (n=2)	M	30
Van Kessel *et al.* [1999]	t(3;4)(p13;p16)	N/a	Clear cell	N/a	M	52
Eleveld *et al.* [2001]	t(3;6)(q11.2;q13)	N/a	Clear cell	Unilateral	F	59
			Clear cell	Unilateral	F	41
			Clear cell	Unilateral	F	63
			Clear cell	Unilateral	M	67
Kanayama *et al.*	t(1;3)(q32;q13.3)	N/a	Clear cell	Unilateral (n=1)	F	79

[2001]

			Clear cell	Bilateral (n=4)	M	56
			Clear cell *	Unilateral (n=1)	M	70
			Clear cell	Unilateral (n=1)	M	62
Podolski *et al.* [2001]	t(2;3)(q33;q21)	N/a	Clear cell	N/a	M	45
			Clear cell	N/a	M	38
			Clear cell *	N/a	M	51
			Clear cell *	N/a	F	51
			Clear cell *	N/a	F	51
			Clear cell *	Bilateral	M	51
			Clear cell *	N/a	F	63
Meléndez *et al.* [2003]	t(3;8)(p14.1;q24.23)	N/a	Clear cell	Bilateral (n=2)	M	46
			Clear cell	Bilateral (n=N/a)	F	56
			Clear cell *	N/a	M	68
			Clear cell	Bilateral (n=N/a)	M	25
			Clear cell	Bilateral (n=N/a)	M	66
			Clear cell	Bilateral (n=N/a)	M	82
			Clear cell	Bilateral (n=N/a)	M	44
			Clear cell	Bilateral (n=N/a)	F	39
			Clear cell	Unilateral (n=N/a)	F	44
Bonne *et al.* [2007]	t(3;15)(p11;q21)	N/a	Clear cell	N/a	F	49
	ins(3;13)(p24.2;q32q21.2)		Clear cell	N/a	N/a	74
Foster *et al.* [2007]	t(3;6)(q22;q16.2)	N/a	Clear cell Papillary	Bilateral (n=3)	M	49
Poland *et al.* [2007]	t(3;8)(p14;q24.1)		Clear cell	Bilateral (n=N/a)	F	47
			Clear cell	Bilateral (n=N/a)	M	39
Kuiper *et al.* [2009]	t(3;4)(q21;q31)	chr3:127177526 chr4:152360211	Clear cell	N/a	N/a	45
McKay *et al.* [2010]	t(2;3)(q37.3;q13.2)	N/a	Clear cell	Bilateral (n=8)	M	54

			Clear cell	N/a	M	50
			Clear cell	Unilateral (n > 1)	F	35
Doyen *et al.* [2012]	t(11;22)(q23-24;q11.2-12)	N/a	Clear cell	Unilateral (n=1)	M	72
Wake *et al.* [2013]	t(5;19)(p15.3;q12)	chr5:6456877-6456885 chr19:29788529-29788531	Oncocytoma Chromophobe	Unilateral (n=2)	F	35
			Clear cell Chromophobe Oncocytoma	Bilateral (n>2)	F	36

Table 2. Clinical details of families harbouring RCC-related translocations cases in this series

Chromosomal alteration	Individual	Carrier	Sex	Age	Histology (RCC)	Type (foci = n)	Sanger	Breakpoints	Additional notes
t(2;17)(q21.1;q11.2)	Proband	Yes	M	37	Clear cell	N/a	Yes	chr2:130693727 chr17:28031855	Some areas of spindle cell changes
	Paternal grandfather	Unknown	M	N/a	Not specified	N/a		N/a	N/a
	Mother	Yes	F	58	Unaffected	N/a		N/a	N/a
	Sibling 1	Yes	?	40	Unaffected	N/a		N/a	N/a
	Sibling 2	Yes	?	31	Unaffected	N/a		N/a	N/a
t(3;6)(p14.2;p12)	Proband	Yes	M	72	Not specified	N/a	Yes	chr3:66680663 chr6:54817716	N/a
	Relative 1	Yes	?	55	Clear cell	Bilateral (n=N/a)	No		Unilateral recurrent RCC and an adrenal metastasis, age 74 years
	Relative 2	Yes	?	N/a	Not specified				
	Relative 3	Yes	?	N/a	Unaffected				Last follow up 47-52 years
	Relative 4	Yes	?	N/a	Unaffected				Last follow up 47-52 years
	Relative 5	Yes	?	N/a	Unaffected				Last follow up 47-52 years
inv(3)(p14.2q12)	Proband	Yes	F	N/a	Unaffected	N/a	No	chr3:59964935 chr3:98667603	

	Cousin	Yes	M	39	Clear cell	N/a			
	Paternal aunt	Yes	F	N/a	Unaffected				
	Father	Yes	M	N/a	Unaffected				
	Grandfather	Yes	M	N/a	Unaffected				Carcinomatosis aged 80 years
	Brother	N/a	M	48	Not specified	N/a			
t(3;14)(q13.3;q23)	Proband	Yes	M	75	Clear cell	n = 2	Yes	chr3:125771297 chr14:59009871	Bladder carcinoma age 77 years
	Nephew	Yes	M	67	Not specified	N/a	Yes	chr3:125771297 chr14:59009871	
	Brother	Obligate	M	79	Not specified	N/a	No	N/a	
	Daughter	Unknown	F	36	Not specified	N/a	No	N/a	
	Brother	Unknown	M	41	Not specified	N/a	No	N/a	
	Mother	Unknown	F	50	Not specified	N/a	No	N/a	
t(10;17)(q11.21;p11.2)	Proband	Yes	M	53	Clear cell	N/a	Yes	N/a	Fibrofolliculomas, pneumothoraces
	Relative	Yes	F	N/a	Unaffected	N/a		N/a	Fibrofolliculomas, multiple lung and renal cysts

Table 3: Details of cytogenetic karyotype, NGS-derived cytogenetic positions, and standardised nomenclature for chromosomal alterations described in this series.

Karyotype	NGS – short nomenclature	NGS – detailed nomenclature
t(3;14)(q13.3;q22)	seq[GRCh38/hg38]t(3;14)(q21;q23)	seq[GRCh38/hg38]t(3;14) (3pter→3q21(125,771,297)::14q23(59009871~59,009,875)→14qter; 14pter→14q23(59009871~59,009,875)::3q21(125,771,298)→3qter)
t(3;6)(p14.2;p12)	seq[GRCh38/hg38]t(3;6)(p14.1;p12.1)	seq[GRCh38/hg38]t(3;6) (3pter→p14.1(66,680,663)::6p12.1(54,817,717)→6qter; 6pter→6p12.1(54,817,716)::3p14.1(66,680,664)→3qter)
inv(3)(p21.1q12)	seq[GRCh38/hg38]inv(3)(p14.2q12)	seq[GRCh38/hg38]inv(3) (qter→q12(98,667,604)::p14.2(59,964,936-98,667,603)::p14.2(59,964,935)→pter)
t(2;17)(q21;q11.2)	seq[GRCh38/hg38]t(2;17)(q21.1;q11.2)	seq[GRCh38/hg38]t(2;17) (2pter→2q21.1(130,693,728)::17q11.2(28,030,856)→17qter; 17pter→17q11.2(28,030,855)::2q21.1(130,693,729)→2qter)
t(10;17)(q11.22;p12)	seq[GRCh38/hg38]t(10;17)(q11.21;p11.2)	seq[GRCh38/hg38]t(10;17) (10pter→10q11.21(43,731,495~43,731,506)::17q11.2(17,121,528~17,121,531)→17qter; 17pter→17q11.2(17,121,525~17,121,530)::10q11.21(43,731,498~43,731,507)→10qter)

Table 4. Reassessment of genes disrupted by translocation breakpoints in RCC-associated translocations reported previously. Genes were categorised according to their current status in NCG v6.0 (Repana *et al.* 2019)

Original publication	Affected genes	Position (GRCh38)	Known cancer gene (NCG 6.0)
Cohen *et al.* [1979]	*FHIT*	chr3:59747587-61251459	Known cancer gene
Cohen *et al.* [1979]	*RNF139 (TRC8)*	chr8:124474738-124488618	Non-cancer gene
Kovacs *et al.* [1989]	*STXBP5*	chr6:147204358-147390476	Non-cancer gene
Koolen *et al.* [1998]	*SLC49A4 (DIRC2)*	chr3:122794795-122881139	Non-cancer gene
van Kessel *et al.* [1999]	*KCNIP4*	chr4:20728606-21948801	Non-cancer gene
Kanayama *et al.* [2001]	*LSAMP*	chr3:115802363-117139389	Non-cancer gene
Kanayama *et al.* [2001]	*RASSF5 (NORE1)*	chr1:206507530-206589448	Non-cancer gene
Podolski *et al.* [2001]	DIRC1	chr2:188733738-188839420	Non-cancer gene
Kuiper *et al.* [2009]	*FBXW7*	chr4:152320544-152536095	Known cancer gene
Wake *et al.* [2013]	UBE2QL1	chr5:6437347-6496721	Non-cancer gene

Table 5: Reassessment of genes highlighted as being close to translocation breakpoints in RCC-associated translocations reported previously. Genes were categorised according to their current status in NCG v6.0 (Repana *et al.* 2019)

Original publication	Affected genes	Position (GRCh38)	Known cancer gene (NCG 6.0)
Meléndez *et al.* [2003]	LRIG1	chr3:66378797-66501263	Candidate cancer gene
Wake *et al.* [2013]	CCNE1	chr19:29811898-29824312	Known cancer gene
Kuiper *et al.* [2009]	C3orf56	chr3:127193131-127198185	Non-cancer gene
Foster *et al.* [2007]	PPP2R3A	chr3:135965673-136147891	Non-cancer gene
Foster *et al.* [2007]	PCCB	chr3:136250306-136337896	Non-cancer gene
Foster *et al.* [2007]	STAG1	chr3:136336233-136752403	Known cancer gene
Foster *et al.* [2007]	MSL2 (RNF184)	chr3:136148922-136197241	Non-cancer gene
Foster *et al.* [2007]	EPHB1	chr3:134597801-135260467	Non-cancer gene
Foster *et al.* [2007]	EPHA7	chr6:93240020-93419547	Non-cancer gene
Podolski *et al.* [2001]	HIBCH	chr2:190189735-190344193	Non-cancer gene
Podolski *et al.* [2001]	INPP1	chr2:190343470-190371665	Non-cancer gene
Podolski *et al.* [2001]	HNRNPC (HNRPC)	chr14:21209136-21269494	Non-cancer gene
Koolen *et al.* [1998]	HSPBAP1	chr3:122740003-122793824	Non-cancer gene
Koolen *et al.* [1998]	SEMA5B	chr3:122909082-123028605	Candidate cancer gene
Yusenko *et al.* [2010]	PDZRN3	chr3:73382433-73624940	Candidate cancer gene
Yusenko *et al.* [2010]	CNTN3	chr3:74262568-74521140	Non-cancer gene

Yusenko *et al.* [2010]	*NECTIN3* (*PVRL3*)	chr3:111070071-111275563	Non-cancer gene
Yusenko *et al.* [2010]	*HSPB8*	chr12:119178642-119221131	Candidate cancer gene
Yusenko *et al.* [2010]	*CCDC60*	chr12:119334712-119541047	Non-cancer gene
Cohen *et al.* [1979]	*TRMT12*	chr8:124450820-124462150	Non-cancer gene
Cohen *et al.* [1979]	*TATDN1*	chr8:124488485-124539458	Non-cancer gene

Table 6. Assessment of genes disrupted by (*) or within the same topologically associating domain as RCC-associated rearrangement reported in the current series. Genes were categorised according to their current status in NCG v6.0 (Repana *et al.* 2019)

Chromosomal alteration	Chr.	Start	End	TAD chr.	TAD start	TAD end	Cancer genes
inv(3)(p21.1q12)	chr3	59964935	59964935	chr3	59920000	61400000	*FHIT *[1]*
	chr3	98667603	98667603	chr3	98600000	99800000	*ST3GAL6 [2]*
t(10;17)(q11.22;p12)	chr17	17218211	17218214	chr17	16840000	18400000	*FLCN *[1]* *LLGL1 [2]*
	chr10	43236047	43236050	chr10	41680000	46360000	*NCOA4 [1]* *RASGEF1A *[2]* *RET [1]*
t(2;17)(q21.1;q11.2)	chr2	130693728	130693728	NA	N/A	N/A	N/A
	chr17	28030855	28030855	chr17	27640000	28360000	*LYRM9 [2]* *TMEM199 [2]*
t(3;14)(q13.3;q22)	chr3	125771297	125771297	NA	N/A	N/A	N/A
	chr14	59009871	59009871	chr14	58440000	59080000	N/A
t(3;6)(p14.2;p12)	chr6	54817716	54817716	chr6	53720000	55240000	N/A
	chr3	66680663	66680663	chr3	66240000	66880000	*LRIG1 [2]*

[1] Known cancer gene; [2] Candidate cancer gene

Figure legends

Figure 1

Circos plots visualising constitutional chromosomal rearrangements. Previously published translocations shown in blue and rearrangements identified in this study shown in orange. Width of the region at the ends of each ribbon represents the proportion of each chromosome which is translocated with its corresponding translocation partner. 1A contains all previously published translocations and translocations in the current series. 1B contains only previously published translocations. 1C contains only rearrangements in this series.

Figure 2

Diagram illustrating the position of chromosome 3 translocation breakpoints across the p and q arms. Differentially shaded portions represent different cytobands, the red region represents the centromeric region. Positions given in cases without base pair resolution are the median position for a given cytoband in the translocation karyotype.
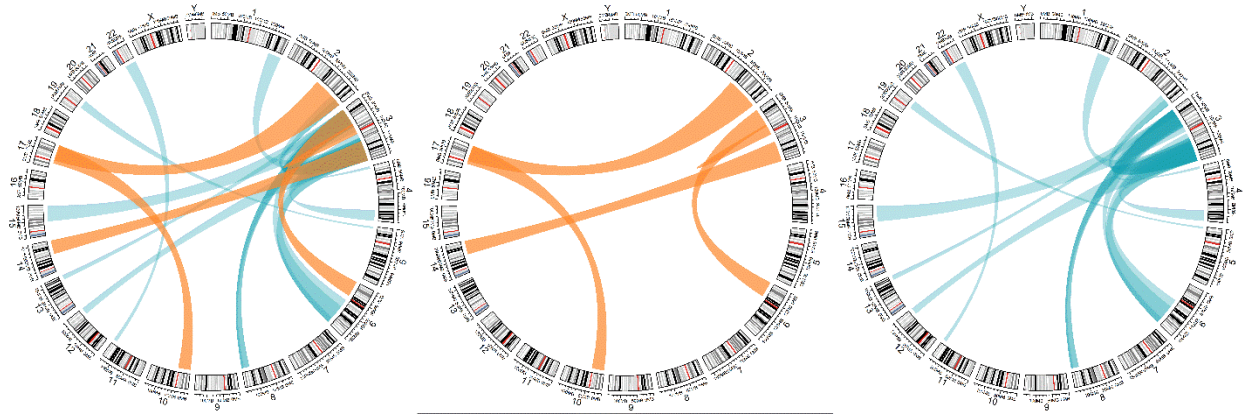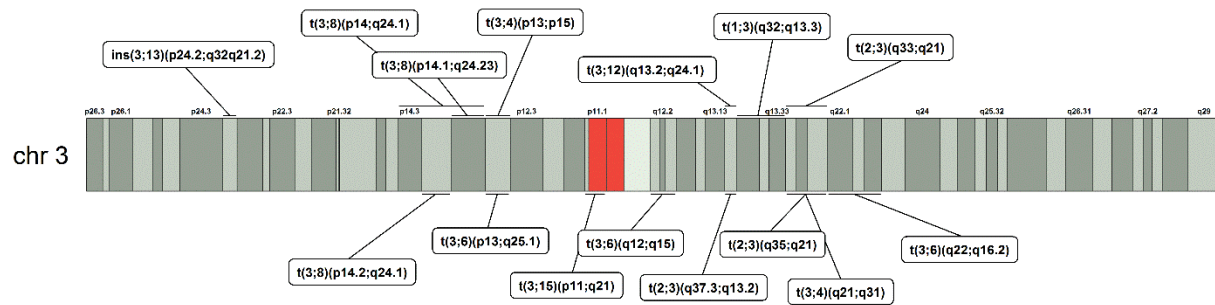
Figure 1

Figure 2